

THERMOGRAVIMETRIC INVESTIGATIONS OF NICKEL-OXIDE THIN FILMS AND POWDERS

R. Cerc Korošec and P. Bukovec

Faculty of Chemistry and Chemical Technology, Aškerčeva 5, SI-1000 Ljubljana, Slovenia

Abstract

Classical TG analysis of films supported on micro-cover glasses was performed in order to determine the appropriate processing temperature to achieve electrochemically active NiO_xH_y thin films. As deposited films made from three different precursors (Ni-acetate, nitrate and sulphate) and their corresponding powders were also investigated. From dynamic TG measurements the onset decomposition temperature could be determined. It was found out that the starting temperature of the mass change of thin films is approximately 30 degrees lower than that of the powders. A broader decomposition range was also observed for thin films. Furthermore, the isothermal treatment of films deposited on conducting substrate at 270 and 300°C was performed and by cyclic voltametry the importance of temperature and time of heating was proved. Films obtained at higher temperatures (>300°C) are electrochemically inert because of the NiO phase formation.

Keywords: nickel oxide, supported films, thermogravimetric analysis

Introduction

TG analysis is a very powerful method, which can also be used for studying the chemical properties of thin films. The standard procedure for performing TG analysis on thin films is to separate them from substrate, because of the enormous dilution effect caused by substrate. The problems appear when films adhere very strongly to substrate and when they are very thin (thickness ≈ 100 nm) [1]. The mass changes of supported films are in the range of buoyancy and aerodynamic effect and are difficult to be measured even by balances in TG instruments which sensitivity is in order of 1 μg (enough to detect thermal decomposition of thin films) [1]. Lieb *et al.* [2] solved this problem by a homemade TG system which allows the use of large-area sample ($1 \times 5-9$ cm^2) and Gallagher [3] succeeded in determining the content of carbon film on fused silica fibre.

To obtain electrochromic NiO_xH_y thin films sol-gel route and dip-coating technique were used. Then deposited films are exposed to higher temperature in order to improve its adherence to substrate and structural stability during potential cycling. TG analysis of supported films was performed in order to determine the appropriate processing temperature to obtain electrochemically active NiO_xH_y thin films. The nanostructure of NiO_xH_y thin films can be most simply described as a layer type configuration in which slabs of NiO_2 are separated by galleries in which various mobile

guest species can reside. In the beginning of the electrochemical cycling a substantial amount of water is intercalated between the adjacent slabs. Weak van der Waals type of bonding allows the entry of species from the electrolyte into the gallery space during cycling [4].

Electrochromism of Ni-oxide films is well documented [5] and it is generally accepted that the transition from a bleached to a coloured state is related to the redox process $\text{Ni}^{2+} \leftrightarrow \text{Ni}^{3+}$. The whole reaction is proposed as a deintercalation of protons: $\text{Ni}(\text{OH})_2 \leftrightarrow \text{NiOOH} + \text{H}^+ + \text{e}^-$ [5]. Temperatures higher than 300°C were found to drastically decrease electrochromic properties of films [6], which was explained by the compacting of the film structure during the formation of an anhydrous NiO. It was also found out that processing temperatures higher than 300°C resulted in electrochemically inert NiO phase when started from nickel nitrate or nickel acetate precursor [7]. For films which were thermally treated to a lesser extent, a decrease of the structure compactness during potential cycling was observed.

No transmittance measurements were done during cycling, but it was proved that electrochemically active films also change their colouration during cycling [6].

Experimental

Preparation of sols, powders (xerogels) and films

Sols were prepared from a nickel nitrate hexahydrate (nickel acetate tetrahydrate and nickel sulphate heptahydrate). In this article only nitrate precursors thin films and powders will be described in detail.

The precipitation of 0.5 M nickel salt (Kemika, Zagreb, Croatia) was carried out with 2 M LiOH (Kemika) until pH 9 was reached. The green precipitate was washed with water and peptised with glacial acetic acid to pH 4.5. Some water was added to obtain appropriate viscosity and sol was then sonificated and filtered [7].

Films for TG measurements were made using a dip-coating technique (pulling velocity 5 cm min⁻¹) on micro-cover glasses and object glasses (1×2 cm²) into which a small hole was previously drilled. A surface active agent (Etolat TD-60, 1 mass% in distilled water, TEOL Factory, Ljubljana, Slovenia) was used as a wetting agent.

Films for cyclovoltametric measurements were deposited on SnO₂/F conducting glasses and surface active agent teloksid (Teloksid A-30, 1 mass% in ethanol, TEOL Factory, Ljubljana, Slovenia) was used.

To obtain the corresponding powders, some amount of sol was air-dried.

Instrumental

Thermoanalytical measurements were carried out in a dynamic air atmosphere using a Perkin Elmer TGA7 Thermoanalyser. Pt crucibles (diameter 8 mm) and heating rate 5°C min⁻¹ was used in dynamic measurements up to 400°C. Sample mass was from 6.72 to 7.54 mg.

Micro-cover glasses (2.2×2.2 cm²) with deposited films were cut with a diamond knife to dimensions suitable for placing into the pan.

In isothermal measurements furnace was heated very fast ($80^{\circ}\text{C min}^{-1}$ up to 200°C) and then heating rate was slowing down ($2^{\circ}\text{C min}^{-1}$ last 10 degrees of heating before isothermal treatment).

Seven-point calibration was performed on TG apparatus using ferromagnetic standards (Alumel, Nickel, Nicoseal, Perkalloy, Trafoperm and Iron), the seventh known temperature was room temperature (22°C).

DTA analysis was made on Perkin Elmer DTA7 instrument in alumina crucible. Heating rate was $10^{\circ}\text{C min}^{-1}$. Sample mass was 8.32 mg and empty alumina crucible was used as a reference. Before the measurement two point calibration was performed, using onset melting temperatures of indium and lead.

EGA measurements were performed on STA 409 Netzsch apparatus. Evolved gases were detected using Laybold Mercous Quadrex 200 Mass Spectrometer. The initial mass of the sample was 500 mg. Heating rate $4^{\circ}\text{C min}^{-1}$, purge gas Ar/O_2 (volume ratio 80:20) and 3.4 ml alumina crucible was used.

Powder diffraction data was obtained using a Phillips PW 1710 X-ray diffractometer with CuK_α radiation from 2 to $70\ 2\theta$ in steps of $0.035^{\circ}\ 2\theta$ and time per step $1\ \text{s}^{-1}$. Qualitative phase analysis was performed using a powder diffraction file.

The thickness of the films was measured using a Surface Profiler Alfa Step 200 with a maximum resolution of 0.5 nm/100 nm.

Cyclovoltametric measurements were performed on EG&G PAR Model 273 computer-controlled potentiostat-galvanostat, driven by 270 Electrochemical Analysis software. The working electrode was SnO_2/F glass $R=20\ \Omega\ \text{cm}^{-1}$ coated with a Ni-oxide film. Samples with dimensions $1\times 3\ \text{cm}^2$ were placed in the cell and equipped with Pt counter and $\text{Ag}/\text{AgCl}/\text{KCl}$ sat. reference electrode. The cell was filled with 40 ml 0.1 M LiOH and for 15 min purged with argon. The scan rate used for cyclic voltametry was $20\ \text{mV s}^{-1}$.

Results

TG analysis of powders and thin films

The solid xerogels always consisted of two phases – dark green and light green, disorderly placed as islands of one in another. Proportion of the phases varied in a wide range. Phases were optically separated and powder diffraction analysis was made for each of them. The former is found to be, regardless to precursor, nickel acetate tetrahydrate and the latter one was amorphous.

Nickel acetate tetrahydrate (crystalline phase) decomposes in two steps (Fig. 1). In the first step from 80 to 175°C the mass change was 27.9%. This value is in good agreement with the calculated value of 28.95% corresponding to lose of 4 molecules H_2O per mole substance. In the second step from 310 to 335°C a decomposition of nickel acetate to nickel oxide occurs. The observed mass change 37.4% is lower than the calculated one (42.3%). IR spectrum of the gray-black residue shows the presence of carbonate and acetate groups. The difference between the antisymmetric ($1507\ \text{cm}^{-1}$) and symmetric ($1436\ \text{cm}^{-1}$) stretching vibration indicates the presence of bidentately chelated acetate groups [8] (Fig. 2).

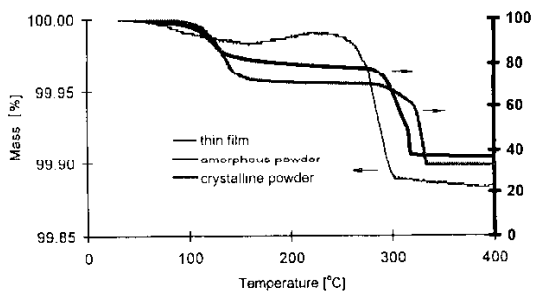


Fig. 1 Dynamic TG curves of crystalline and amorphous powders and that of thin film

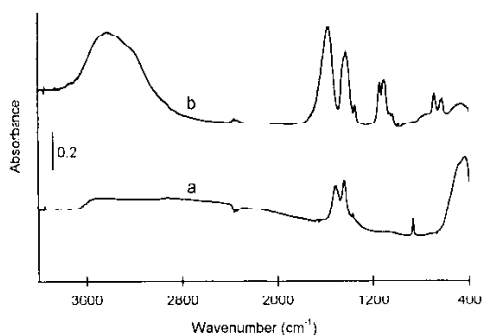


Fig. 2 IR spectra of the a) amorphous powder (made from nickel nitrate precursor) heat treated in air to 400°C, b) amorphous powder made from sulphate precursor and exposed to air at 300°C for 15 min

Decomposition of amorphous phases depends on precursor used. For nitrate precursor the first step occurs in the range from 80 to 160°C due to endothermic reaction (as seen from DTA curve) with a mass loss of 20%. From EGA measurements it is evident that only water molecules (adsorbed or intercalated) are released from the sample, meaning that the first step is dehydration. The second decomposition step starts at 195°C and results in a 39% mass change. From DTA curve (Fig. 3) it is clearly seen that two successive reactions take place in this range, which is also in accordance with the EGA measurements. The evolved gases in the first less exothermic reaction are only CO and CO₂, while in the second one also water was present.

In TG measurements of thin films the initial mass (micro cover glass+thin film) was in the range from 97.262 to 139.623 mg. Thickness of the films was in the range from 75 to 130 nm. The mass change in the former was 0.022 mg in the first step (50–160°C) and 0.085 mg in the second one (266–300°C). For heavier sample the mass loss was 0.154 mg in the second step. In dynamic measurements slight buoyancy effect was observed (mass gain 0.006 mg) in the temperature range from 150 to

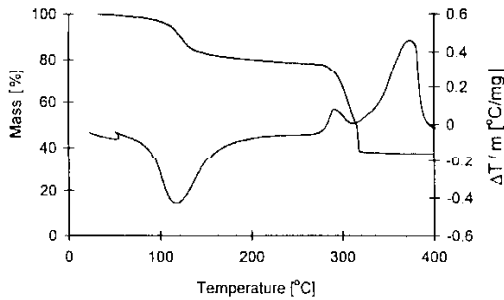


Fig. 3 TG and DTA curves of the amorphous phase

250°C where no decomposition reaction takes place. In Fig. 1 the TG curves of crystalline and amorphous powders and thin films are presented.

Micro-cover glass with wetting agent was also investigated. The obtained TG curve was identical as for glass only – meaning that no decomposition reaction happens in the agent in the studied temperature range.

In dynamic measurements of thin films an excellent reproducibility and high resolution was obtained even though overall mass change was only 0.15% (Fig. 4).

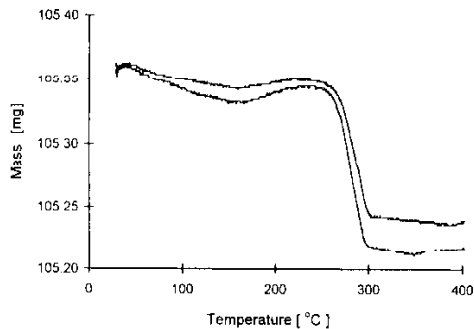


Fig. 4 Reproducibility of TG measurements on thin films

Furthermore sol was deposited on small object glass ($1 \times 2 \text{ cm}^2$), which was then hanged on platinum wire. The initial mass was 320.927 mg and only 0.007 mg mass change was monitored. The resolution was thus very poor, but the same onset decomposition temperature was found for film on object glass and for films on micro-cover glass placed in a pan.

It is easy to calculate the percent of the mass change during heating when studying powdered samples. Here once again the problem appears when thin films are investigated. We tried to determine the initial mass of the film deposited on small object glass from mass difference by carefully weighing the glass+film and glass on

TG balance, but the obtained results were difficult to interpret. It happens that the overall mass was smaller than that of the substrate. We supposed therefore that the total mass change in percent is the same in the film as in powder when exposed to 400°C. This assumption allowed us to calculate the initial mass of the film, which was in the range of 0.145 to 0.210 mg. In the Figs 2–4 overall mass changes (film+glass) are used.

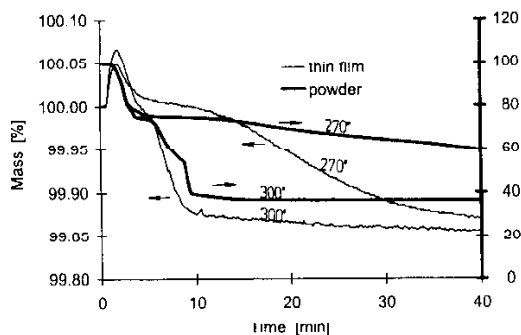


Fig. 5 Isothermal TG curves of powders and thin films in flowing air at 270 and 300°C

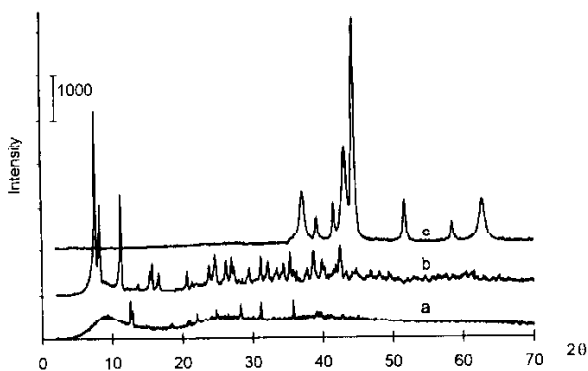


Fig. 6 XRD spectra of a – the amorphous phase, b – amorphous phase heat treated in air at 270°C, c – amorphous phase heat treated at 300°C

In isothermal treatment the furnace reached the final temperature in 7 min. The actual temperature was 6 degrees higher than programmed one. For CV measurements films were exposed to 270 or 300°C for 15 min. The isotherms of the films were then compared to isotherms of powders obtained at same conditions after 22 min (Fig. 5). During this time, amorphous powder losses its mass very slowly to 60%. It seems that in the second step only one reaction occurs. At the same temperature film fully decomposes in about 40 min but reactions progress slowly and with

time it is possible to control the decomposition of the film. When both film and powder are exposed to 300°C, decomposition is finished in 3 min, although the slight mass change with time occurred for thin film. At this temperature it is impossible to control the amount of formed NiO.

Powder diffraction data results

Powder diffraction results show that amorphous powders still contain some nickel acetate tetrahydrate (Fig. 6). When exposed for 15 min to 270°C, they transform partly to nickel hydroxide hydrate, lithium acetate hydrate and lithium nitrate. Two large interplanar distances ($d=11.517$ and 10.644 Å) with high intensity were observed and could be attributed to turbostratic layered structure [9]. At 300°C powders transform to NiO bunsenite phase, but also nickel nitride was found in the residue.

Cyclovoltametric results

The CV response of the film ($d=85$ nm) cycled between -0.4 to 0.7 V vs. Ag/AgCl reference electrode is shown in Fig. 7.

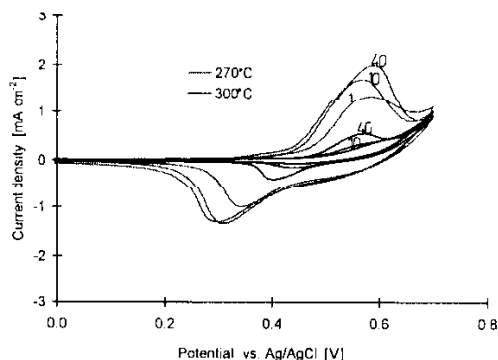


Fig. 7 Cyclovoltametric curves of Ni-oxide film ($d=85$ nm) heat treated in air at 270 and 300°C

In the first cycle the oxidation peak occurs at 0.58 V for film exposed to 270°C for 15 min. During the reverse scan maximum reduction process is observed at 0.34 V. The corresponding current densities are 1.3 mA cm^{-2} in oxidizing and -1.0 mA cm^{-2} in reducing directions, respectively. During the subsequent cycles (40 V) a slight shift of anodic peak towards higher potentials (0.59 V) and cathodic peaks towards lower values (0.30 V) were obtained. This indicates the decrease of the film compactness with increasing number of cycles [7].

Film exposed to 300°C is electrochemically inert. During the cycling hydration and hydroxylation processes [7] lead to formation of more porous phase, which also exhibits small oxidation ($E=0.57$ V; $I=0.6 \text{ mA cm}^{-2}$) and reduction ($E=0.40$ V; $I=-0.4 \text{ mA cm}^{-2}$) peaks.

Table 1 Comparison between decomposition temperatures of thin film and corresponding powders made from three different precursors

Precursor	Onset temp. for the beginning of the mass change/ $^{\circ}\text{C}$	Difference between onset decomposition temp. for thin film and powder/ $^{\circ}\text{C}$	End temp. of the decomposition/ $^{\circ}\text{C}$	Difference between starting and ending decomposition temp./ $^{\circ}\text{C}$
acetate	265	35	302	32
powder	300		331	23
nitrate	266	29	300	34
powder	295		323	30
thin film	295	32	350	55
powder	327		361	34

Conclusions

Dynamic TG measurements are very important in processing electrochemically active NiO_xH_y phases. High resolution TG curves were obtained for films deposited on micro-cover glasses, even though the mass ratio substrate/film was close to 460. Three different films made of nickel nitrate, nickel acetate and nickel sulphate precursor start to decompose approx. 30 degrees lower than amorphous powders. This is attributed to a very small particle size [10] of the substance, deposited within the thin film. Nitrate and acetate films and powders behave very similar. On the contrary, sulphate precursor leads to higher decomposition temperature. These results are in accordance with thermal stability of corresponding salts [11]. The results obtained by dynamic measurements are given in Table 1. For thin films the larger decomposition range was observed because the diffusion of the evolved gases during the decomposition is suppressed by glass at one side.

At 270°C amorphous powders irrespectively to precursor lose mass slowly from 80 to 60%. Corresponding amorphous powder reflects turbostratic structure, which ensures a higher diffusion coefficient for the proton due to the presence of the layer of water molecules [9]. At the same temperature nitrate and acetate films fully decompose in about 40 min, but reaction progresses slowly and with time it is possible to control decomposition extent of these two films. The formation of electrochemical inert phase is confirmed by the presence of stretching $\nu(\text{Ni}-\text{O})$ mode at 460 cm^{-1} . Nitrate film processed at 270°C is electrochemically active. Sulphate film at 270°C decomposes similarly to corresponding powder, meaning that only dehydration occur. For sulphate precursor a decrease of cyclovoltametric response was observed during potential cycling.

When both films and powders made from acetate and nitrate precursors are exposed to 300°C, decomposition is finished in 3 min. Films are electrochemically inert because the formation of NiO phase is predominant. Water molecules are released from the structure, which becomes too compact to intercalate proton. During subsequent cycling, slow recuperation of the structure occurs. At this temperature decomposition reaction for sulphate film is not finished even in 40 min, meaning that film is still electrochemically active. IR spectra of powders show that the formation of NiO begins, but sulphate anions remain free between layers and partly monodentately bonded to nickel cations (Fig. 2).

References

- 1 M. Leskelä, T. Leskelä and L. Niinistö, *J. Thermal Anal.*, 40 (1993) 1077.
- 2 S. Lieb, R. K. McCrone, J. J. Theimer and E. W. Maby, *J. Mater. Res.*, 1 (1986) 792.
- 3 P. K. Gallagher, *J. Thermal Anal.*, 38 (1992) 17.
- 4 R. A. Huggins, H. Prinz, M. Wohlfahrt-Mehrens, L. Jürissen and W. Witschel, *Solid State Ionics*, 70/71 (1994) 417.
- 5 C. G. Granqvist, *Handbook of Inorganic Electrochromic Materials*, Elsevier Oxford, 1995, Chapter 19.
- 6 M. C. A. Fantini, G. H. Bezerra, C. R. C. Carvalho and A. Gorenstein, *Proc. SPIE* 1536 (1991) 81.

- 7 A. Surca, B. Orcl, B. Pihlar and P. Bukovec, *J. Electroanal. Chem.*, 408 (1996) 83.
- 8 K. Nakamoto, *Infrared and Raman Spectra of Inorganic and Coordination Compounds*, Wiley New York, 1977.
- 9 C. Faure, C. Delmas and M. Fouassier, *J. Power Source*, 35 (1991) 279.
- 10 W. W. Wendlandt, *Thermal Methods of Analysis*, Wiley, New York, 1974, Chapter 2.
- 11 *Atlas of Thermoanalytical Curves*, Ed. by G. Liptay, Vol. 1, 2, 3, 5, Akadémiai Kiadó Budapest, 1977.